Organic & Biomolecular Chemistry

This article is part of the

OBC 10th anniversary

themed issue

All articles in this issue will be gathered together online at

www.rsc.org/OBC10

Organic & Biomolecular Chemistry

Cite this: *Org. Biomol. Chem.*, 2012, **10**, 6087

www.rsc.org/obc

PAPER

Amphiphilic dynamic NDI and PDI probes: imaging microdomains in giant unilamellar vesicles†‡

David Alonso Doval, Andrea Fin, Miwa Takahashi-Umebayashi, Howard Riezman, Aurelien Roux, Naomi Sakai and Stefan Matile*

Received 16th January 2012, Accepted 28th February 2012
DOI: 10.1039/c2ob25119a

Dynamic amphiphiles provide access to transmembrane ion transport, differential sensing and cellular uptake. In this report, we introduce dynamic amphiphiles with fluorescent tails. Core-substituted naphthalenediimides (cNDIs) and perylenediimides (cPDIs) are tested. Whereas the latter suffer from poor partitioning, dynamic cNDI amphiphiles are found to be purifiable by RP-HPLC, to partition selectively into liquid-disordered (Ld) microdomains of mixed lipid bilayers and to activate DNA as transporters. Importantly, fluorescence properties, partitioning and activity can be modulated by changes in the structure of mixed amphiphiles. These results confirm the potential of dynamic fluorescent amphiphiles to selectively label extra- and intracellular membrane domains and visualize biological function.

Introduction

Dynamic amphiphiles are amphiphiles that contain dynamic bonds or "bridges" to connect hydrophilic heads and lipophilic tails.[1–4] Although emphasis has so far been on hydrazone bridges, there is much potential in introducing other dynamic covalent bonds such as disulfides, boronic esters or oximes to build chemoorthogonal bridges in dynamic amphiphiles. Dynamic amphiphiles are of interest with regard to ion transport in vesicles[1–3] and applications to cellular uptake[4] as well as biosensing, aptamerosensing and differential sensing of analytes of free choice.[1] They have originally been introduced to expand biosensing applications with synthetic transport systems to also include lipophilic analytes such as cholesterol.[2] However, dynamic amphiphiles soon turned out to be most attractive for differential sensing with synthetic transport systems. In brief, hydrophobic analytes such as muscone **1** are covalently captured *in situ* with reactive head groups like **2**, that is simple glutamate derivatives containing one guanidinium cation and two hydrazides each (Fig. 1a).[1] The resulting dynamic amphiphile **3** with two hydrazone bridges is then characterized as activator of DNA transporters in fluorogenic vesicles (Fig. 1c, e). Different activities with different head groups are used to generate patterns which are then recognized by principal component or hierarchical cluster analysis. Differential sensing with dynamic

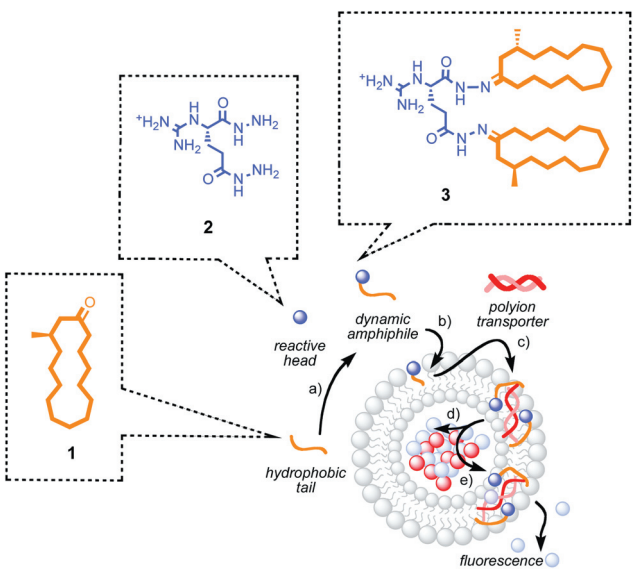

Fig. 1 Dynamic amphiphiles as fluorescent membrane probes (b), for cellular uptake (c, d) transport (c, e), and sensing (a, c, e). Hydrophobic "tails" (*e.g.*, muscone **1**) are covalently captured by hydrophilic cations (*e.g.*, dihydrazide **2**) to give dynamic amphiphiles (*e.g.*, **3**) that can partition into lipid bilayer membranes (b) and activate polyanions (*e.g.*, DNA, c) for cellular uptake (d) or cation transport in fluorogenic vesicles ((e), shown here is the example of fluorescence recovery in response to the export of trapped cationic quenchers (blue) but not anionic fluorophores (red)).

School of Chemistry and Biochemistry, University of Geneva, Geneva, Switzerland. E-mail: stefan.matile@unige.ch; www.unige.ch/sciences/chiorg/matile/; Fax: +41 22 379 5123; Tel: +41 22 379 6523

† This article is part of the *Organic & Biomolecular Chemistry* 10th Anniversary issue.

‡ Electronic supplementary information (ESI) available: Detailed experimental procedures. See DOI: 10.1039/c2ob25119a

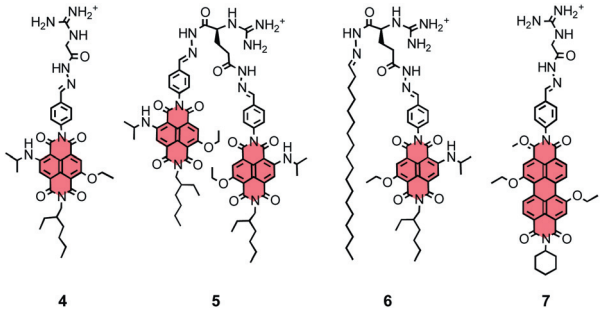

Fig. 2 Fluorescent dynamic cNDI and cPDI amphiphiles introduced in this study. All cNDIs are mixtures of 3,7- and 2,6-regioisomers in the core and epimers in the alkyl tail (compare Fig. 4).

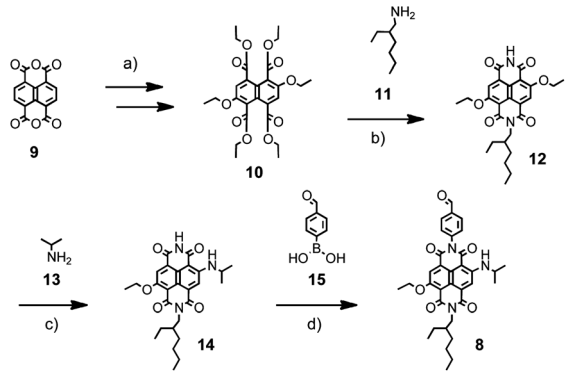

Scheme 1 Synthesis of red cNDI tail **8**. (a) 1. Dibromoisocyanuric acid; 2. EtI, EtOH, K_2CO_3, 35%; 3. NaOEt, 73%; (b) 1. KOH, iPrOH, reflux, 15 h; 2. **11**, AcOH/H_2O 1 : 1, 160 °C, μW, 5 min; 3. ammonium acetate, AcOH/H_2O 1 : 1, pH 4, 160 °C, μW, 30 min, 15%; (c) **13**/DCM 1 : 1, rt, 22 h, 72%; (d) $Cu(OAc)_2$, TEA, DMAc, O_2, 55 °C, 20 h, 62%. **8** and **14** are mixtures of 3,7- and 2,6-regioisomers and mixtures of enantiomers, 4 isomers each in total.

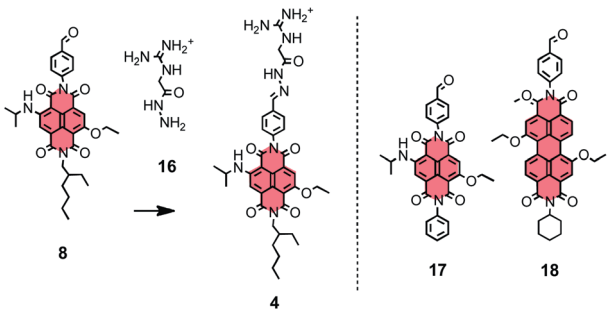

Fig. 3 Covalent capture of aldehyde substrates as single-tail dynamic amphiphiles.

amphiphiles has been exemplified with artificial noses for odorants or perfumes as illustrative samples from the supermarket.[1]

For cellular uptake, dynamic amphiphiles are attractive because they provide effortless access to significant libraries.[4] With design principles largely obscure, screening will be essential to tackle significant current challenges such as the delivery of siRNA[5] or understanding and control over the mode of action of cell-penetrating peptides.[6] Preliminary results in this direction are encouraging.[4]

In this report, a third general application of dynamic amphiphiles is envisioned for the first time, *i.e.*, fluorescent membrane probes.[7–9] Hydrophobic by nature, the poor delivery of dedicated fluorescent membrane probes often hampers their usefulness in practice.[8] Dynamic probes have the potential that their properties can be tailored on demand. This includes delivery not only to the extracellular membrane, but also to intracellular locations assisted by polyion transporters.[1–4] Moreover, the release of dynamic probes at membranes of interest is conceivable by fine tuning the reactivity of the bridge, and targeting and positioning could be modulated further in mixed multitail amphiphiles.

To test these ideas, we selected core-substituted naphthalenediimide (cNDI)[10,11] and perylenediimide (cPDI)[12,13] fluorophores as examples (Fig. 2). Little explored as membrane probes, these fluorophores were considered promising because their long lifetime is interesting for single-molecule studies, their ability to cover the full visible range without global structural changes is ideal for FRET applications,[10] and their compact planar structure promised partitioning into more ordered membrane domains.[9,13] We report the design, synthesis and evaluation of dynamic NDI and PDI amphiphiles, including mixed systems. We show that they can be separated and purified by RP-HPLC, activate DNA as transporters, and that their partitioning into liquid disordered (Ld) phase can be modulated in mixed amphiphiles and used to label microdomains in GUVs.

Results and discussion

The red, fluorescent tails **8** were accessible from naphthalene dianhydride **9** in seven steps (Scheme 1).[14] The conversion of substrate **9** into the core-substituted naphthalene tetraester **10** was accomplished in three steps following published procedures.[10] From there, the esters were hydrolyzed with base and the product reacted first with racemic 2-ethyl-1-hexylamine **11** and then with ammonium acetate. Microwave-assisted imide formation gave the mixed diimide **12** together with the symmetric side products.

Core substitution with *iso*-propylamine **13** converted the yellow cNDI **12** into the red cNDI **14**. In the final step, a Cu-catalyzed C–N bond formation was employed to couple **14** and boronic acid **15**. Structure and homogeneity of the final product **8** was confirmed by NMR spectroscopy, mass spectrometry (MS) and high-pressure liquid chromatography (HPLC).

The dynamic NDI amphiphile **4** with one single fluorescent tail was obtained by incubation of aldehyde **8** with the cationic monohydrazide **16**[1] for 1 h in dry DMSO at 60 °C (Fig. 3).[1–3] The originally envisioned aldehyde **17** could not be used for this purpose because it was insoluble in DMSO and other applicable solvents. The dynamic homologue **7** with a single PDI tail was obtained by incubation of PDI aldehyde **18** under identical conditions (Fig. 3). The synthesis of cPDI **18** with two ethoxy groups in the core is described in the ESI.‡[14]

One advantage with fluorescent tails was that formation and stability of dynamic amphiphiles could be more easily followed by reverse-phase (RP) HPLC.[14] Single-tail amphiphiles **4** and **7** were identified and purified by this method, and their structure was confirmed by electrospray ionization (ESI) MS. However,

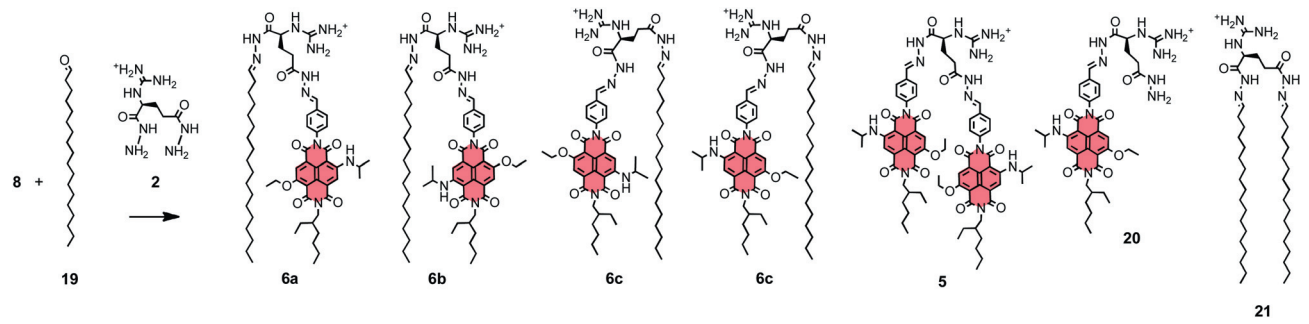

Fig. 4 Covalent capture of aldehyde substrates as double-tail dynamic amphiphiles. All four regioisomers of mixed amphiphile **6** are shown, they all exist as pairs of epimers. Analogous regio- and stereoisomers for **5** and **20** are not shown.

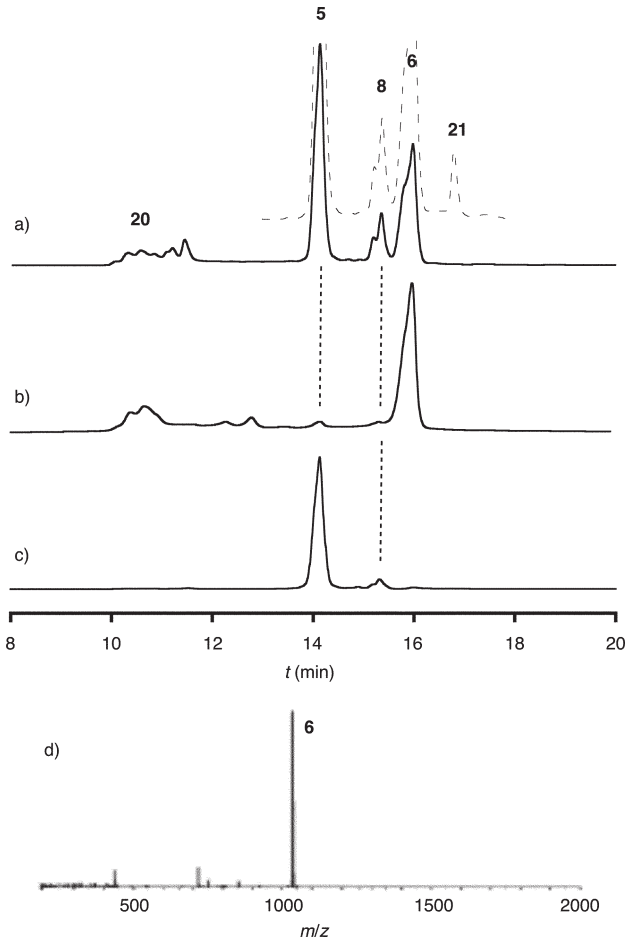

Fig. 5 PR-HPLC traces of (a) the crude reaction mixture obtained from covalent capture of aldehydes **8** and **19** by dihydrazide **2**, (b) purified mixed amphiphile **6** and (c) purified di-NDI **5** with detection by absorption at 540 nm (solid) and at 250 nm (dashed); (d) ESI MS of **6**.

HPLC analysis was most interesting with double-tail amphiphiles because mixed systems could be included. Incubation of cNDI aldehyde **8** together with the cationic dihydrazide **2**[1] as well as octadecyl aldehyde **19** gave reasonably complex RP-HPLC profiles (Fig. 4 and 5a). Best results were obtained on a YMC-Pack OSD-A S-5 µm column (120A C18, 250 mm × 10 mm) and a gradient elution moving from 4 : 6 to 7 : 1 THF–water with 0.1% TFA within 12 min at a flow rate of 3 ml min^{-1}. Under these conditions, cNDI **8**, the starting material, appeared with a retention time t_R = 15.3 min (Fig. 5a). The split peak indicated that 2,6- and 3,7-regioisomers could be separated. This separation of regioisomers has already been accomplished with similar samples.[15]

The dynamic amphiphile **5** with two NDI tails appeared at t_R = 14.1 min (Fig. 5a). Isolation of the sample and reinjection was possible with negligible hydrolysis of the hydrazone bridges (Fig. 5c). Traces of free aldehyde **8** appeared (<5%), whereas the broad peaks of single tail intermediates **20** around t_R ~ 11 min remained undetectable. The dynamic amphiphile **21** with two alkyl tails was visible at 250 nm (Fig. 5a). The mixed amphiphiles **6** appeared at t_R = 15.9 min as a broad peak with a shoulder. The product **6** was quite stable during isolation and characterization. A dominant single peak was obtained for pure material by ESI MS (Fig. 5d). Reinjection of purified material gave mixed amphiphiles **6** as dominant product, confirming stability during purification, also under acidic conditions (Fig. 5b). In HPLCs of purified samples, the broad peak for single-tail degradation products around t_R ~ 10.2 min decreased with decreasing acidity of the acid used during purification by HPLC (*i.e.*, 15% with 0.1% TFA, pK_a 0.50; 8% with 0.1% formic acid, pK_a 3.75; 4% with 0.1% acetic acid, pK_a 4.76). The amphiphiles **20** with single NDI tails appeared as main side products, confirming that aryl hydrazone bridges are more stable than alkyl hydrazones. Interestingly, the dynamic amphiphile **5** with two NDI tails appeared as well as a minor side product. This finding pointed toward the occurrence of tail scrambling during purification and characterization.

To illustrate the beauty and power of the approach, we prepared also the dynamic amphiphile **22** with three NDI tails by incubating aldehyde **8** with trihydrazide **23**[1] (Fig. 6). Eluted at t_R = 16.0 min, triple-tail amphiphile **22** could be isolated, reinjected and subjected to ESI MS without significant tail loss. Mixed triple-tail amphiphiles were not prepared because mixed double-tail amphiphiles **6** were sufficient to outline the functional benefits of tail mixing.

The ability of dynamic amphiphiles **4**, **6** and **7** to activate DNA as cation transporter in lipid bilayer membranes was determined under established conditions.[1–3] Fluorogenic large unilamellar vesicles (LUVs) were prepared by swelling dried egg yolk phosphatidylcholine (EYPC) films in water containing buffers, an anionic fluorophore (HPTS, 8-hydroxy-1,3,6-pyrenetrisulfonate) and a cationic quencher (DPX, *p*-xylene-bispyridinium bromide). The obtained EYPC LUVs ideally report the export of DPX quenchers by counterion activated DNA as an

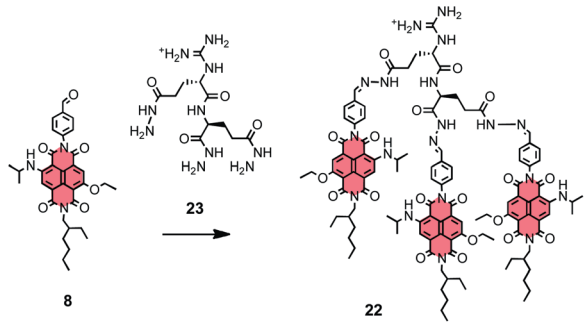

Fig. 6 Covalent capture of aldehyde substrates as triple-tail dynamic amphiphiles.

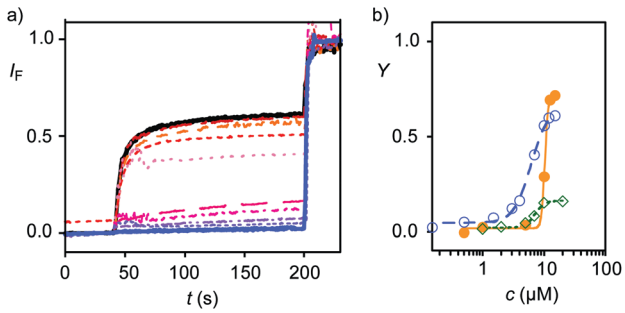

Fig. 7 (a) Changes in fractional fluorescence intensity I_F of HPTS (λ_{ex} = 413 nm, λ_{em} = 510 nm) during addition of increasing concentrations of mixed amphiphile **6** ($t \sim 0$ s), ctDNA (1.25 μg ml^{-1} final concentration, $t \sim 40$ s) and excess triton X-100 ($t \sim 200$ s) to EYPC-LUVs⊇HPTS/DPX. (b) Dose response curves for ctDNA activated by dynamic counterions **4** (●), **6** (○) and **7** (◇) with fit to the Hill equation.

increase in the emission of the ratiometric fluorophore HPTS. In reality, fluorescence recovery in this assay can originate from the export of cationic DPX, anionic HPTS or both from intact vesicles, or from the destruction of the vesicles. However, internal trapping experiments have shown that counterion activation enables DNA to move across intact lipid bilayers, and DPX but not HPTS transport across bulk chloroform membranes has been confirmed experimentally.[16]

The addition of either amphiphile **4**, **6** or **7** (Fig. 7a, $t < 40$ s) or calf thymus (ct) DNA to the vesicles did not cause a significant fluorescence response. However, both together, **4**, **6** or **7** and ctDNA, caused fluorescence recovery (Fig. 7a, $t > 40$ s). This finding indicated that amphiphiles **4**, **6** and **7** activate ctDNA transporters in EYPC LUVs. The intensity before lysis (Fig. 7a, $t = 200$ s) was taken as fractional activity Y and plotted as a function of activator concentration at constant DNA concentration (Fig. 7b). Hill analysis gave Y_{MAX}, the maximal accessible activity under these conditions, the EC_{50}, the effective activator concentration needed to reach 50% of Y_{MAX}, and the Hill coefficient n, which indicates the steepness of the sigmoidal fitting (Table 1).

All activators functioned with a very satisfactory $EC_{50} \sim 8$ μM. With single-tail NDI amphiphile **4**, the highest EC_{50} coincided with highest Y_{MAX} = 72% as well as highest n = 17 (Table 1, entry 1). This exceptional cooperativity indicated that at least 17 amphiphiles **4** are needed to activate DNA, and that the resulting active polyion-counterion complexes are thermodynamically unstable.[17] A poor Y_{MAX} = 16% suggested that single-tail PDI amphiphiles **7** and/or their stable complexes with polyions prefer to precipitate rather than partition into the EYPC membrane (Table 1, entry 3). Decreasing EC_{50} = 7.2 μM and n = 5.7 were in agreement with this interpretation. An improvement to EC_{50} = 6.2 μM and n = 3.1 without significant losses in Y_{MAX} = 66% was possible with the mixed double-tail NDI amphiphile **6** (Table 1, entry 2). This attractive behavior suggested that the alkyl tail in amphiphile **6** improves the stability of the active complexes without losses in their partitioning into EYPC membranes.

With fluorescent tails as intrinsic probes, the partitioning of dynamic NDI and PDI amphiphiles could be determined directly. Because their fluorescence is quenched in water, partitioning in lipid bilayers was detectable as fluorescence recovery at 575 nm (Fig. 8a). Partitioning into 1,2-dioleoyl-*sn*-glycero-3-phosphocholine (DOPC) LUVs in liquid disordered (Ld) phase was tested first. The obtained response to increasing DOPC concentrations was fitted to

$$I = I_{MIN} + (I_{MAX} - I_{MIN})/(1 + [H_2O]/K_x\,[\text{lipid}]) \quad (1)$$

where I is the fluorescence response, $I_{MIN} = I$ without lipids, $I_{MAX} = I$ at saturation, $[H_2O]$ the concentration of water (55.3 M), and K_x the partition coefficient.[18] With $K_x \sim 15\,000$, both NDI amphiphiles **4** and **6** partitioned well into DOPC LUVs (Table 1, entries 1 and 2). Fluorescence recovery of PDI amphiphile **7** was not detectable above scattering, a finding that was consistent with the poor Y_{MAX} = 16% for DNA activation (Table 1, entry 3).

Partitioning of NDI amphiphile into the solid-ordered (So) phase of 1,2-dipalmitoyl-*sn*-glycero-3-phosphocholine (DPPC) LUVs and the liquid-ordered (Lo) phase of DPPC/cholesterol

Table 1 Transport and partitioning data[a]

Cpd[b]	Y_{MAX} (%)[c]	n[d]	EC_{50} (μM)[e]	K_x DOPC[f]	K_x DPPC[g]	K_x DPPC/CL[h]	K_x DOPC/CL[i]
4	71.6 ± 2.4	17.1 ± 1.2	10.3 ± 0.1	(1.6 ± 0.5) 10^4	(7.8 ± 4.5) 10^3	(2.2 ± 1.4) 10^3	(6.1 ± 2.6) 10^3
6	66.0 ± 3.0	3.1 ± 0.4	6.2 ± 0.3	(1.3 ± 0.5) 10^4	(2.2 ± 0.9) 10^3	(4.1 ± 1.1) 10^3	(8.8 ± 3.8) 10^3
7	16.3 ± 0.9	5.7 ± 1.6	7.2 ± 0.4	—	—	—	—

[a] From HPTS/DPX assay (Y_{MAX}, n, EC_{50}, Fig. 7) and fluorescence recovery of NDI tails in membranes (Fig. 8). [b] Compounds (Fig. 2). [c] Maximal activity accessible relative to full vesicles destruction. From Hill analysis of dose response curves (Fig. 7b). [d] Hill coefficient. [e] Effective concentration, concentration needed to reach 50% of Y_{MAX}. [f–i] Partition coefficient K_x in LUVs of different composition (Fig. 8); DOPC, 1,2-dioleoyl-*sn*-glycero-3-phosphocholine; DPPC, 1,2-dipalmitoyl-*sn*-glycero-3-phosphocholine; CL, cholesterol.

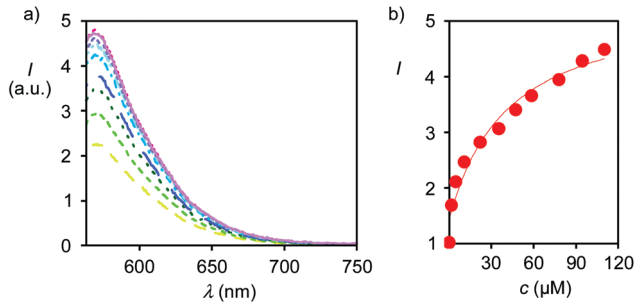

Fig. 8 (a) Increase in fluorescence emission intensity I_F of mixed NDI amphiphile **6** (λ_{ex} = 540 nm) in the presence of increasing concentrations of DOPC LUVs. (b) Dose response curve for data in (a), showing emission I at 575 nm as a function of DOPC concentration with curve fit to eqn (1).

(CL) LUVs was clearly less favorable and more difficult to detect above scattering. With all due caution, it can be said that single-tail amphiphile **4** preferred the So phase (K_x = 7800) over the Lo phase (K_x = 2200). This trend was reversed with addition of an octadecyl tail in mixed double-tail NDI amphiphile **6**, which showed some preference for the Lo phase (K_x = 4100) over So phase (K_x = 2200). Insensitivity in DOPC/CL LUV controls suggested that the observed trends are valid. The addition of a saturated alkyl tail was thus sufficient to increase the partitioning into the Lo phase but clearly insufficient to "push" the mixed amphiphile **6** from the Ld phase (K_x = 13 000) into the Lo phase (K_x = 4100).

Partitioning of fluorescent NDI and PDI probes into mixed LUVs with different microdomains was not determined because fluorescence spectroscopy cannot differentiate between the microdomains and the results would be as for microdomain-free vesicles and thus meaningless. To more qualitatively probe for selective partitioning within mixed membranes, confocal imaging of giant unilamellar vesicles (GUVs) is the method of choice (Fig. 9).[7,19] The larger GUVs are required for detection by fluorescence microscopy. One of the most reliable compositions of GUVs to study microdomains is SM–DOPC–CL 56 : 24 : 20.[7i] Under these optimized conditions, it is possible to quite frequently observe GUVs that show separation into Lo and Ld phases at room temperature, a situation that is perfect for unambiguous data analysis. Egg sphingomyelin (SM) and CL form the microdomains in the Lo phase, whereas DOPC segregates into the separate microdomains in the Ld phase. Compared to standard experiments in LUVs described above, DPPC is thus replaced by SM to form, together with cholesterol, the Lo microdomains in the GUVs.

In heterogeneous GUVs composed of SM–DOPC–CL 56 : 24 : 20, Lo phases can be labeled with 0.05 mol% naphthopyrene, a fluorescent probe that emits blue light. The fluorescent probe BODIPY FL C5-HPC can be used alternatively to selectively label the Ld domains. The partitioning of the new NDI probes **4–6** in mixed GUVs was explored under these standard conditions. For this purpose, GUVs composed of SM/DOPC/CL 56 : 24 : 20 were prepared in the presence of 0.1–0.5 mol% of an NDI probe and 0.05 mol% naphthopyrene. Confocal microscopy z-scanning was recorded simultaneously for red emission from NDI probes (λ_{ex} 543 nm) and blue emission from naphthopyrene

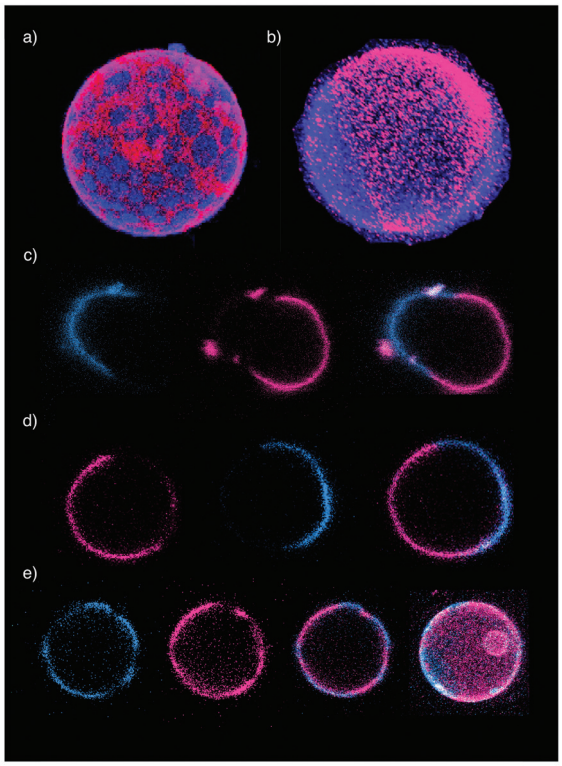

Fig. 9 Fluorescent images of GUVs composed of SM/DOPC/CL 56 : 24 : 20 with 0.1–0.5 mol% of (a, b) **4**, (c) **5** and (d, e) **6** (red emission, λ_{ex} 543 nm) and 0.05 mol% naphthopyrene in the Lo phase (blue emission, λ_{ex} 405 nm). Single plane images of the equator region show simultaneously recorded red and blue emission separately (c–e, left) and merged (c–e, right). Complete GUVs were reconstructed from z-scans in 0.8 μm increments (a, b and e, far right). The diameters of all shown GUVs were around ~10 μm, their dispersity covered roughly one order of magnitude.

in the Lo phase (λ_{ex} 405 nm). Single plane images obtained at the equatorial region of the GUVs revealed little overlap of the blue and the red fluorescence (Fig. 9c–e, left side). Merging of the individual z-stacks fully confirmed the impression that the blue and red fluorescence do not overlap (Fig. 9c–e, right side). Full images of complete GUVs were constructed from serial confocal optical sections at 0.8 μm intervals (Fig. 9a, 9b and 9e, far right). The most revealing smaller GUVs with two to three large domains were observed most frequently (Fig. 9b–d). Smaller GUVs with several domains were seen less frequently (Fig. 9e). Multiple domains in a single, usually larger GUV were only found occasionally (Fig. 9a).

Coexisting Ld and Lo phases were observed for all GUVs, and the blue and red fluorescence never overlapped strongly. Knowing that naphthopyrene partitions into the Lo phase composed of SM and CL, this finding demonstrated that in heterogeneous SM–DOPC–CL GUVs, the new NDI probes partition into the Ld phase composed of DOPC. Overlapping emission

with green-fluorescent BODIPY FL C5-HPC control probes for Ld domains (λ_{ex} 488 nm) corroborated the validity of this interpretation (Fig. S8‡). Uniform partitioning of dynamic NDI amphiphiles into Ld phases in GUVs was consistent with the partition coefficients determined in LUVs (Table 1).

Quantitative determination of differences in partitioning by fluorescence imaging in GUVs is not as straightforward as by fluorescence spectroscopy in LUVs. However, separate single plane images of the equator region indicated that NDIs **4** and **5** with more pronounced preferences for Ld phases left not a shade of red emission in the area occupied by the blue fluorescent Lo phase (Fig. 9c). The increasing acceptance of mixed NDI amphiphiles **6** in Lo phases could be guessed from the appearance of red fluorescence within blue domains (Table 1, entry 2; Fig. 9d, e). However, these qualitative differences between the NDI probes in GUVs are relatively minor and much less evident than in quantitative measurements in LUVs. Controls confirmed that dynamic triple-tail amphiphile **22** suffers increasingly from intramolecular fluorescence quenching but still partitions into the Ld phase (Fig. S8‡). The partitioning of dynamic PDI amphiphiles was too poor for meaningful fluorescence imaging in GUVs.

Conclusions

This is the first report on dynamic amphiphiles with fluorescent tails. NDIs and PDIs were selected as representative fluorophores, mainly for convenience but also because of their potential as photostable FRET systems in Lo phases. The synthesis of NDIs and PDIs with one aldehyde was as straightforward as expected, solubilizing groups had to be added and refined. With fluorescent tails, covalent capture by hydrazide head groups could be easily followed by RP-HPLC. Dynamic NDI amphiphiles could be purified, isolated and characterized without excessive decomposition. Dynamic NDI amphiphiles activated DNA as transporters in lipid bilayers, and activity could be modulated by the composition of the of mixed systems. Dynamic PDI amphiphiles were nearly inactive due to poor partitioning. This finding confirmed that dynamic NDI (but not PDI) amphiphiles could be used to visualize cellular uptake pathways and label intracellular membranes. For example, one can imagine active complexes with DNA being taken up by endocytosis, amphiphilic NDI hydrazones being hydrolyzed in the more acidic endosomes and hydrophobic NDI probes being released to report on the nature of endosomal membranes.

Qualitative imaging in mixed GUVs revealed that dynamic NDI amphiphiles partition into the Ld phase, independent of their structure. However, quantitative partitioning studies in LUVs revealed that partitioning in mixed membranes can be modulated by the composition of mixed amphiphiles. Taken together, these results fully confirm the potential of dynamic fluorescent amphiphiles to selectively label extra- and intracellular membrane domains, and that the selectivity can be modulated with the structure of mixed amphiphiles. With cNDIs and particularly cPDIs not fully convincing, we currently focus on dynamic fluorescent amphiphiles that operate with environmental-sensitive, conceptually innovative fluorophores rather than by partitioning.

Acknowledgements

We thank D. Jeannerat, A. Pinto and S. Grass for NMR measurements, the Sciences Mass Spectrometry (SMS) platform for mass spectrometry services, and the University of Geneva, the European Research Council (ERC Advanced Investigator), the National Centre of Competence in Research (NCCR) Chemical Biology and the Swiss NSF for financial support.

References

1 T. Takeuchi, J. Montenegro, A. Hennig and S. Matile, *Chem. Sci.*, 2011, **2**, 303–307.
2 S. M. Butterfield, T. Miyatake and S. Matile, *Angew. Chem., Int. Ed.*, 2009, **48**, 325–328.
3 (*a*) J. Montenegro, P. Bonvin, T. Takeuchi and S. Matile, *Chem.–Eur. J.*, 2010, **16**, 14159–14166; (*b*) J. Montenegro and S. Matile, *Chem.–Asian J.*, 2011, **6**, 681–689; (*c*) J. Montenegro, A. Fin and S. Matile, *Org. Biomol. Chem.*, 2011, **9**, 2641–2647.
4 (*a*) C. Gehin, J. Montenegro, E.-K. Bang, A. Fin, S. Matile and H. Riezman, in preparation; (*b*) E.-K. Bang and S. Matile, in preparation.
5 (*a*) S. C. Semple, A. Akinc, J. Chen, A. P. Sandhu, B. L. Mui, C. K. Cho, D. W. Y. Sah, D. Stebbing, E. J. Crosley, E. Yaworski, I. M. Hafez, J. R. Dorkin, J. Qin, K. Lam, K. G. Rajeev, K. F. Wong, L. B. Jeffs, L. Nechev, M. L. Eisenhardt, M. Jayaraman, M. Kazem, M. A. Maier, M. Srinivasulu, M. J. Weinstein, Q. Chen, R. Alvarez, S. A. Barros, S. De, S. K. Klimuk, T. Borland, V. Kosovrasti, W. L. Cantley, Y. K. Tam, M. Manoharan, M. A. Ciufolini, M. A. Tracy, A. de Fougerolles, I. MacLachlan, P. R. Cullis, T. D. Madden and M. J. Hope, *Nat. Biotechnol.*, 2010, **28**, 172–176; (*b*) M. Mével, N. Kamaly, S. Carmona, M. H. Oliver, M. R. Jorgensen, C. Crowther, F. H. Salazar, P. L. Marion, M. Fujino, Y. Natori, M. Thanou, P. Arbuthnot, J.-J. Yaouanc, P. A. Jaffrès and A. D. Miller, *J. Controlled Release*, 2010, **143**, 222–232; (*c*) M. E. Davis, J. E. Zuckerman, C. H. J. Choi, D. Seligson, A. Tolcher, C. A. Alabi, Y. Yen, J. D. Heidel and A. Ribas, *Nature*, 2010, **464**, 1067–1070; (*d*) V. Janout and S. L. Regen, *Bioconjugate Chem.*, 2009, **20**, 183–192; (*e*) J. A. Boomer, M. M. Qualls, H. D. Inerowicz, R. H. Haynes, V. S. Patri, J. M. Kim and D. H. Thompson, *Bioconjugate Chem.*, 2009, **20**, 47–59; (*f*) S. Bhattacharya and A. Bajaj, *Chem. Commun.*, 2009, 4632–4656.
6 (*a*) K. Inomata, A. Ohno, H. Tochio, S. Isogai, T. Tenno, I. Nakase, T. Takeuchi, S. Futaki, Y. Ito, H. Hiroaki and M. Shirakawa, *Nature*, 2009, **458**, 106–109; (*b*) P. A. Wender, W. C. Galliher, E. A. Goun, L. R. Jones and T. H. Pillow, *Adv. Drug Delivery Rev.*, 2008, **60**, 452–472; (*c*) A. A. Kale and V. P. Torchilin, *Bioconjugate Chem.*, 2007, **18**, 363–370; (*d*) E. K. Esbjorner, P. Lincoln and B. Norden, *Biochim. Biophys. Acta, Biomembr.*, 2007, **1768**, 1550–1558; (*e*) T. Shimanouchi, P. Walde, J. Gardiner, Y. R. Mahajan, D. Seebach, A. Thomae, S. D. Kraemer, M. Voser and R. Kuboi, *Biochim. Biophys. Acta, Biomembr.*, 2007, **1768**, 2726–2736; (*f*) M. Martinell, X. Salvatella, J. Fernández-Carneado, S. Gordo, M. Feliz, M. Menéndez and E. Giralt, *ChemBioChem*, 2006, **7**, 1105–1113; (*g*) T. Takeuchi, M. Kosuge, A. Tadokoro, Y. Sugiura, M. Nishi, M. Kawata, N. Sakai, S. Matile and S. Futaki, *ACS Chem. Biol.*, 2006, **1**, 299–303; (*h*) T. Jiang, E. S. Olson, Q. T. Nguyen, M. Roy, P. A. Jennings and R. Y. Tsien, *Proc. Natl. Acad. Sci. U. S. A.*, 2004, **101**, 17867–17872.
7 (*a*) T. Baumgart, G. Hunt, E. R. Farkas, W. W. Webb and G. W. Feigenson, *Biochim. Biophys. Acta, Biomembr.*, 2007, **1768**, 2182–2194; (*b*) T. Baumgart, S. T. Hess and W. W. Webb, *Nature*, 2003, **425**, 821–824; (*c*) T. Hamada, R. Sugimoto, T. Nagasaki and M. Takagi, *Soft Matter*, 2011, **7**, 220–224; (*d*) H. M. Kim and B. R. Cho, *Acc. Chem. Res.*, 2009, **42**, 863–872; (*e*) L. A. Bagatolli, *Biochim. Biophys. Acta, Biomembr.*, 2006, **1758**, 1541–1556; (*f*) O. A. Kucherak, S. Oncul, Z. Darwich, D. A. Yushchenko, Y. Arntz, P. Didier, Y. Mely and A. S. Klymchenko, *J. Am. Chem. Soc.*, 2010, **132**, 4907–4916; (*g*) J. Sutharsan, D. Lichlyter, N. E. Wright, M. Dakanali, M. A. Haidekker and E. A. Theodorakis, *Tetrahedron*, 2010, **66**, 2582–2588; (*h*) P. Yan, A. Xie, M. Wei and L. M. Loew, *J. Org. Chem.*, 2008, **73**, 6587–6594; (*i*) N. F. Morales-Penningston, J. Wu, E. R. Farkas, S. L. Goh, T. M. Konyakhina, J. Y. Zheng, W. W. Webb and G. W. Feigenson, *Biochim. Biophys. Acta, Biomembr.*, 2010, **1798**, 1324–1332.

8 J. P. Wuskell, D. Boudreau, M. Wei, L. Jin, R. Engl, R. Chebolu, A. Bullen, K. D. Hoffacker, J. Kerimo, L. B. Cohen, M. R. Zochowski and L. M. Loew, *J. Neurosci. Methods*, 2006, **151**, 200–215.

9 A. Margineanu, J. Hotta, M. Van der Auweraer, M. Ameloot, A. Stefan, D. Beljonne, Y. Engelborghs, A. Herrmann, K. Mullen, F. C. De Schryver and J. Hofkens, *Biophys. J.*, 2007, **93**, 2877–2891.

10 (*a*) N. Sakai, J. Mareda, E. Vauthey and S. Matile, *Chem. Commun.*, 2010, **46**, 4225–4237; (*b*) R. S. K. Kishore, O. Kel, N. Banerji, D. Emery, G. Bollot, J. Mareda, A. Gomez-Casado, P. Jonkheijm, J. Huskens, P. Maroni, M. Borkovec, E. Vauthey, N. Sakai and S. Matile, *J. Am. Chem. Soc.*, 2009, **131**, 11106–11116; (*c*) N. Sakai, M. Lista, O. Kel, S. Sakurai, D. Emery, J. Mareda, E. Vauthey and S. Matile, *J. Am. Chem. Soc.*, 2011, **133**, 15224–15227; (*d*) M. Lista, J. Areephong, N. Sakai and S. Matile, *J. Am. Chem. Soc.*, 2011, **133**, 15228–15230; (*e*) N. Sakai and S. Matile, *J. Am. Chem. Soc.*, 2011, **133**, 18542–18545.

11 (*a*) B. J. H. Oh, S. L. Suraru, W. Y. Lee, M. Könemann, H. W. Höffken, C. Röger, R. Schmidt, Y. Chung, W. C. Chen, F. Würthner and Z. Bao, *Adv. Funct. Mater.*, 2010, **20**, 2148–2156; (*b*) C. W. Marquardt, S. Grunder, A. Błaszczyk, S. Dehm, F. Hennrich, H. V. Löhneysen, M. Mayor and R. Krupke, *Nat. Nanotechnol.*, 2010, **5**, 863–867; (*c*) Y. Hu, X. Gao, C. Di, X. Yang, F. Zhang, Y. Liu, H. Li and D. Zhu, *Chem. Mater.*, 2011, **23**, 1204–1215.S. V. Bhosale, C. H. Jani, C. H. Lalander, S. J. Langford, I. Nerush, J. G. Shapter, D. Villamaina and E. Vauthey, *Chem. Commun.*, 2011, **47**, 8226–8228.

12 (*a*) F. Würthner, *Chem. Commun.*, 2004, 1564–1579; (*b*) S. Foster, C. E. Finlayson, P. E. Keivanidis, Y.-S. Huang, I. Hwang, R. H. Friend, M. B. J. Otten, L.-P. Lu, E. Schwartz, R. J. M. Nolte and A. E. Rowan, *Macromolecules*, 2009, **42**, 2023–2030; (*c*) A. D. Shaller, W. Wang, H. Gan and A. D. Q. Li, *Angew. Chem., Int. Ed.*, 2008, **47**, 7705–7709; (*d*) M. M. Safont-Sempere, P. Osswald, M. Grüne, M. Renz, M. Kaupp, K. Radacki, H. Braunschweig and F. Würthner, *J. Am. Chem. Soc.*, 2011, **133**, 9580–9591; (*e*) J. M. Giaimo, A. V. Gusev and M. R. Wasielewski, *J. Am. Chem. Soc.*, 2002, 124, 8530–8531.

13 (*a*) A. Perez-Velasco, V. Gorteau and S. Matile, *Angew. Chem., Int. Ed.*, 2008, **47**, 921–923; (*b*) S. Bhosale, A. L. Sisson, P. Talukdar, A. Fürstenberg, N. Banerji, E. Vauthey, G. Bollot, J. Mareda, C. Röger, F. Würthner, N. Sakai and S. Matile, *Science*, 2006, **313**, 84–86.

14 See ESI.‡.

15 R. Bhosale, R. S. K. Kishore, V. Ravikumar, O. Kel, E. Vauthey, N. Sakai and S. Matile, *Chem. Sci.*, 2010, **1**, 357–368.

16 T. Takeuchi, V. Bagnacani, F. Sansone and S. Matile, *ChemBioChem*, 2009, **10**, 2793–2799.

17 S. Bhosale and S. Matile, *Chirality*, 2006, **18**, 849–856.

18 S. H. White, W. C. Wimley, A. S. Ladokhin and K. Hristova, *Methods Enzymol.*, 1998, **295**, 62–87.

19 (*a*) P. Walde, K. Cosentino, H. Engel and P. Stano, *ChemBioChem*, 2010, **11**, 848–865; (*b*) F. M. Menger and J. S. Keiper, *Curr. Opin. Chem. Biol.*, 1998, **2**, 726–732.